

Winds in collision: high-energy particles in massive binary systems

Sean M. Dougherty* †

National Research Council Herzberg Institute for Astrophysics, Canada

E-mail: sean.dougherty@nrc.ca

Julian M. Pittard

Physics and Astronomy, University of Leeds, UK

E-mail: jmp@ast.leeds.ac.uk

High-resolution radio observations have revealed that non-thermal radio emission in Wolf-Rayet (WR) stars arises where the stellar wind of the WR star collides with that of a binary companion. These colliding-wind binary (CWB) systems offer an important laboratory for investigating the underlying physics of particle acceleration. Hydrodynamic models of the binary stellar winds and the wind-collision region (WCR) that account for the evolution of the electron energy spectrum, largely due to inverse Compton cooling, are now available. Radiometry and imaging obtained with the VLA, MERLIN, EVN and VLBA provide essential constraints to these models. Models of the radio emission from WR146 and WR147 are shown, though these very wide systems do not have defined orbits and hence lack a number of important model parameters. Multi-epoch VLBI imaging of the archetype WR+O star binary WR140 through a part of its 7.9-year orbit has been used to define the orbit inclination, distance and the luminosity of the companion star to enable the best constraints for any radio emitting CWB system. Models of the spatial distribution of relativistic electrons and ions, and the magnetic energy density are used to model the radio emission, and also to predict the high energy emission at X-ray and γ -ray energies. It is clear that high-energy facilities e.g. GLAST and VERITAS, will be important for constraining particle acceleration parameters such as the spectral index of the energy spectrum and the acceleration efficiency of both ions and electrons, and in turn, identify unique models for the radio spectra. This will be especially important in future attempts to model the spectra of WR140 throughout its complete orbit. A WCR origin for the synchrotron emission in O-type stars, the progenitors of WR stars, is illustrated by observations of Cyg OB2 #9.

The 8th European VLBI Network Symposium

September 26-29 2006

Toruń, Poland

*Speaker.

†This work has been done in collaboration with Perry Williams (U. Edinburgh, UK), Sven Van Loo (U. Leeds, UK), Tony Beasley (ALMA), Ronny Blomme (Royal Observatory, Belgium), Evan O'Connor (UPEI, Canada) and Nick Bolingbroke (U. Victoria, Canada)

1. Wind-collision regions and particle acceleration

Wolf-Rayet (WR) stars have dense stellar winds that are photo-ionized by the strong UV radiation fields from the underlying WR star, giving rise to a free-free continuum emission spectra, observable from IR to radio wavelengths. The brightness temperature of this emission is $\sim 10^4$ K, as expected from a photo-ionized envelope in thermal equilibrium. The emission is partially optically thick with a power-law spectrum $S_\nu \propto \nu^\alpha$, with a spectral index (α) typically $\sim +0.7$ between mid-IR and radio frequencies e.g. [28]. However, a number of WR stars have radio emission properties that differ from this typical picture: they exhibit high brightness temperatures ($\sim 10^6 - 10^7$ K), and have flat or negative spectral indices, properties characteristic of non-thermal synchrotron emission and high-energy phenomena in the stellar winds [1, 2].

Spatially resolved observations of the WR+O binary systems WR 147 [15, 27] and WR 146 [8, 9] presented the first unequivocal confirmation that the synchrotron emission did not arise within the stellar wind of a single star, but at the location of the wind-collision region (WCR) where the stellar winds of two massive stars collide – the colliding-wind binary (CWB) model [10] (Fig. 1). This model is further supported by the dramatic variations of the synchrotron radio emission in the 7.9-year WR+O binary system WR 140, that are clearly modulated by the binary orbit (c.f. Fig. 4). A CWB origin for the synchrotron emission in WR stars was first proposed by [23]. This has now been substantiated with over 90% of WR stars that exhibit non-thermal emission characteristics being found to be either binary or having a “nearby” massive stellar companion resulting in a WCR [7].

Colliding-wind binary systems present an important laboratory for investigating the underlying physics of particle acceleration. In addition to the excellent modelling constraints provided from high resolution VLBI imaging, radiometry and high energy observations, CWBs provide access to higher mass, radiation and magnetic field densities than those found in supernova remnants, which have widely been used for this work.

2. Modelling of wind-collision regions

Models of the radio emission from these systems have been based largely on highly simplified models, in order to maintain analytic solutions of the radiative transfer equation. Today, models based on 2-D hydrodynamical models of the density and pressure distributions in the stellar winds and the WCR are available (Fig. 2), that lead to a description of both the population and the spatial distribution of the relativistic particles in the WCR [6, 18]. In addition to the free-free opacity of the stellar winds, these models account for changes in the intrinsic synchrotron luminosity and the free-free and synchrotron absorption within the WCR. The models assume that the electrons are shock accelerated by the standing shocks on either side of the contact discontinuity of the two stellar winds. Other potential acceleration mechanisms, such as magnetic reconnection (e.g. [12]) have been considered but it has been argued that, although such a mechanism could provide the radio synchrotron luminosity, reconnection may not provide sufficient power for the anticipated flux of non-thermal X-ray emission [17]. At the shocks, the energy distribution of the relativistic electrons is specified by a power law i.e. $n(\gamma) \propto \gamma^{-p}$. As the electrons advect downstream, the spectrum evolves away from a simple power law as the electrons cool via Inverse Compton (IC)

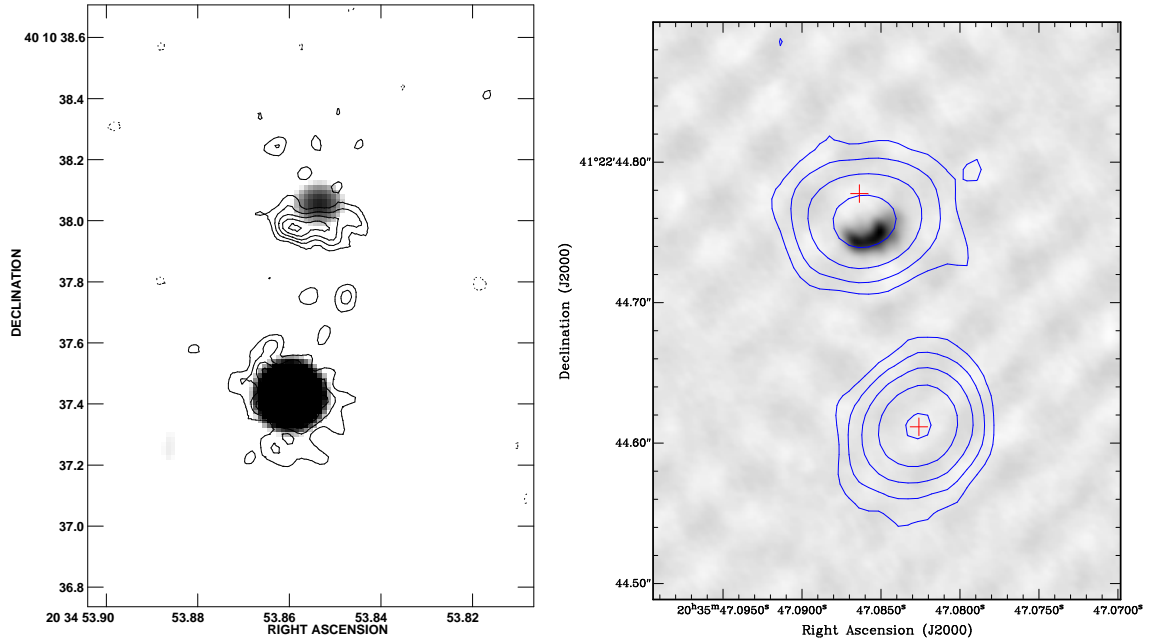


Figure 1: Left: Overlay of a MERLIN 5-GHz image of WR147 (contours) and a $2.2\mu\text{m}$ UKIRT image (greyscale). The IR image of the WR star was aligned with the peak position of the thermal emission in the southern radio component, assumed to be the ionized stellar wind of the WR star. The position of the non-thermal emission region (the northern radio component) is consistent with the location of ram pressure balance between the winds of the WR star and the B-type companion revealed in the IR image [27]. Right: 4.8-GHz EVN (greyscale) and 43-GHz VLA+PT (contours) observations of WR146. The crosses denote the relative positions of the stars determined by HST [15] and assuming the peak of the southern 43-GHz component (thermal emission) is the WR star (from [16]). The northern component is dominated by synchrotron emission, even at 43 GHz c.f. Fig. 3.

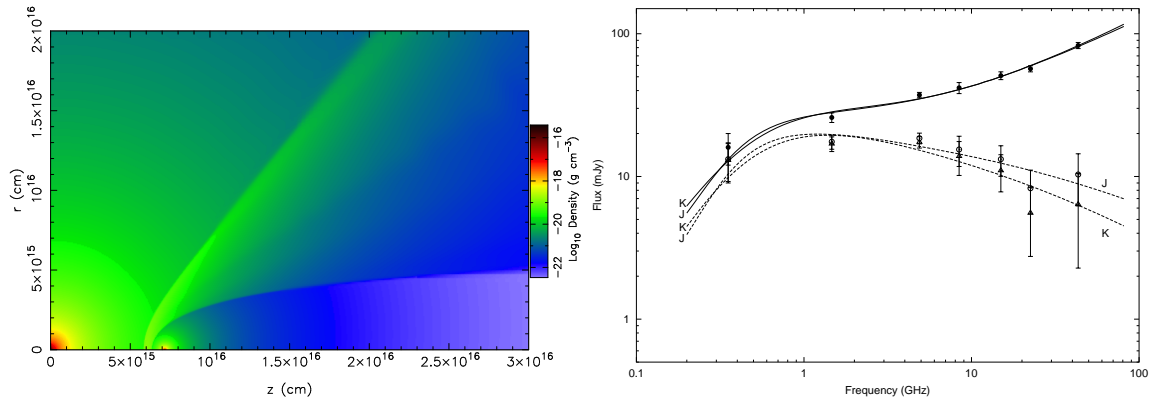


Figure 2: Left: An example of the density distribution in a model of the WR147 CWB system. The WR star is at $(0,0)$ and the O-star companion is at $(7.2 \times 10^{15} \text{ cm}, 0)$. The WCR bounded by two standing shocks on either side of the ram pressure balance surface of the two stellar winds is clearly visible. Right: Radio fluxes from WR147 with model fits to both the total (solid symbols) and the non-thermal emission component (open symbols) based on the 2D-hydrodynamic models of the WCR and stellar winds shown on the left (from [18]).

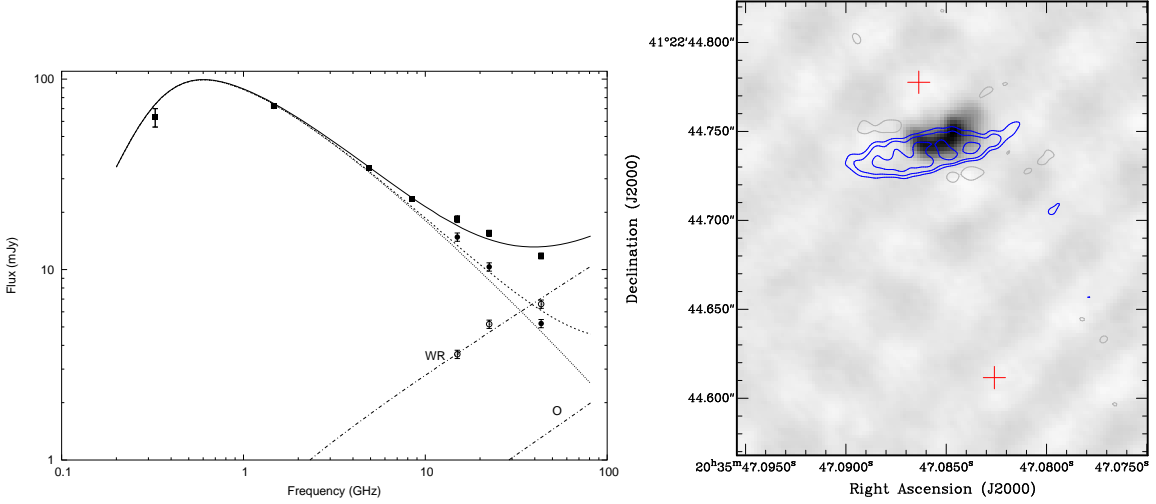


Figure 3: Left: Best-fit models of the radio emission from the WCR in WR146, with synchrotron (dotted), thermal (lower dot-dashed) and synchrotron+thermal (dashed). The thermal emission from the WR star wind is the higher dot-dashed line. The solid line is the total flux. Right: EVN 4.9-GHz observations of the WCR in WR146 (greyscale) with a simulated EVN observation (contours) based on the model shown on the left. The crosses mark the relative location of the two stars (from [16]).

cooling. The non-thermal and magnetic energy densities are both normalized to some fraction of the thermal energy density, with the normalization factors determined by fitting the radio spectrum. These models have been applied with some success to observations of WR147 (Fig. 1) and WR146 (Fig. 3). The models of WR147 are not as well constrained by the available data as those of WR146, since the synchrotron emission does not dominate the total emission from the system, as in WR146. However, in the latter system current models fail to accurately reproduce the spectrum at higher frequencies, and the model WCR emission is more extended than observed by the EVN [16]. In spite of these issues, the value of the modelling constraints posed by both the radiometry and the VLBI imaging is clear.

3. WR140 – the particle acceleration laboratory

In spite of the success of reproducing both the spectra and the spatial distribution of the radio emission, the models of very wide systems such as WR146 and WR147 contain a number of ill-constrained, yet key parameters. These systems do not exhibit radial velocity variations and so do not have defined orbits. The inclination of the system to the line of sight is unknown and hence the geometry of the system, particularly the stellar separation, is unknown. Closer systems with periods of a few years present much better systems for WCR modelling since many orbit parameters are defined, and they maintain optically thin lines of sight to the WCR.

WR140 is the archetype CWB, with a WC7 star and an O4-5 star in a highly elliptical orbit ($e \approx 0.88$). It is well known for the dramatic variations in its emission from near-IR to radio wavelengths [26, 28], and also at X-ray energies during its 7.9-year orbit [19, 20, 30]. The WCR in WR140 experiences significant changes as the stellar separation varies between ~ 2 AU at periastron and ~ 30 AU at apastron. The observed radio emission increases by up to two orders of magnitude

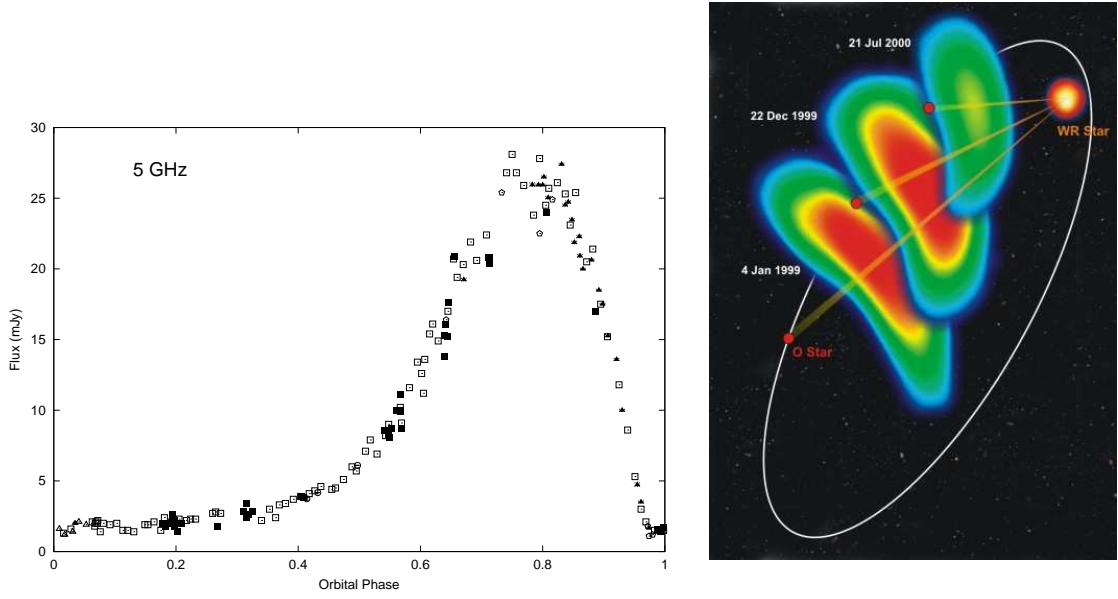


Figure 4: Left: 5-GHz VLA radiometry of WR 140 as a function of orbital phase for orbit cycles between 1978-1985 (pentagons), 1985-1993 (squares), 1993-2001 (triangles), and 2000-2007 (circles). Open symbols are from the VLA [5, 26] and solid symbols from the WSRT [28, 29]. Right: A montage of 8.4-GHz VLBA observations of WR 140 at three orbital phases showing the rotation of the WCR as the orbit progresses. The deduced orbit is superimposed [5].

between periastron and a frequency-dependent peak between orbital phases 0.65 and 0.85, followed by a steep decline. This behaviour repeats from one orbit cycle to another, suggesting a particle acceleration mechanism that is well-controlled by the orbit of the system (Fig. 4). Recent VLBI observations have provided key constraints on a number of critical system parameters, including orbit inclination, distance, and luminosity of the O-star companion, and make WR140 the ideal system for modelling particle acceleration in a WCR.

3.1 Defining the orbit through VLBI observations

To establish the geometry of the WR140 binary system, particularly the orbital inclination (i) and semi-major axis (a), but also the longitude of the ascending node (Ω), the system must be resolved into a “visual” binary. This was achieved with the Infrared-Optical Telescope Array (IOTA) interferometer [14], and together with the established orbit parameters [13], gives families of possible solutions for (i, Ω, a) . Until further interferometric observations are available, VLBI observations of the WCR provide the only means currently to determine uniquely i , and hence Ω and a , from the possible families of IOTA solutions.

A 24-epoch campaign of VLBA observations of WR140 was carried out between orbital phase 0.7 and 0.9 [5]. At each epoch, an arc of emission is observed, resembling the bow-shaped morphology expected for a WCR. This arc rotates from “pointing” NW to W as the orbit progresses. The WCR emission is expected to wrap around the star with the lower wind momentum – the O star. In this case, the rotation of the WCR as the orbit progresses implies that the O star moves from the SE to close to due E of the WR star over the period of the VLBA observations. Thus, the direc-

tion of the orbit is established. Secondly, the orbital inclination can be derived from the change in the orientation of the WCR with orbital phase. Each (i, Ω) family provides a unique set of position angles for the projected line-of-centres as a function of orbital phase. This gives $i = 122^\circ \pm 5^\circ$ and $\Omega = 353^\circ \pm 3^\circ$, leading to a semi-major axis of $a = 9.0 \pm 0.5$ mas, and the first full definition of orbit parameters for *any* CWB system. From optical spectroscopy $a \sin i = 14.10 \pm 0.54$ AU [13], and so the VLBA orbit parameters require a distance of 1.85 ± 0.16 kpc. This distance is independent of a calibration of stellar parameters e.g. absolute magnitude, and implies that the O star is a supergiant.

3.2 Modelling the radio emission from WR140

With the geometry and stellar parameters in WR140 defined, models of the WCR are better constrained than in any other known CWB. In addition, observations of the thermal X-ray emission that arises from the shocked plasma in the WCR provide the best constraints on the mass-loss rates of the two winds as a function of the momentum ratio, η , of the two winds. Any clumps in the stellar wind flows are destroyed by the colliding-wind shocks and the post-shock flow is smooth. Thus, the thermal X-ray emission provides clumping-free mass-loss estimates for the two stars.

Models of the radio and X-ray emission at orbital phase 0.837 have been developed [17]. At this orbital phase, non-thermal emission dominates the radio spectrum, and so a good estimate of the characteristics of the relativistic electrons can be made. Fig. 5 shows two preferred fits to the radiometry, with quite different values of relative wind-momentum. Unfortunately, VLBI arrays do not currently have enough sensitivity to distinguish between these models through determining the asymptotic shock opening angle, but the orbit geometry imposed by the multi-epoch VLBI imaging suggest the model with $\eta \approx 0.02$ is most appropriate.

The models convincingly demonstrate that the turnover at ~ 3 GHz is due to free-free absorption in the winds, since models where the Razin effect dominates the low-frequency spectrum place an unacceptably large fraction of the shock energy in non-thermal electrons. The radio fits also require electron spectra with $p < 2$, i.e. the spectral index of the non-thermal electron energy distribution is flatter than the canonical strong shock value of $p = 2$ expected for diffusive shock acceleration. A number of mechanisms could lead to such an index [17].

3.3 Non-thermal high-energy emission in WR140

Definitive evidence for non-thermal X-ray and γ -ray emission from CWBs does not yet exist, but many of the unidentified EGRET sources appear correlated with populations of massive stars [21]. Notably, WR140 is located in the outskirts of the positional error box of 3EG J2022+4317 and raises the possibility of γ -ray emission from a CWB.

The population of relativistic electrons that give rise to the radio synchrotron emission are also responsible for high energy IC and relativistic bremsstrahlung emission. Thus, model fits to the radio data naturally provide an estimate of the high energy emission from these processes. The detailed treatment of the spatial dependence of the non-thermal electron distribution and magnetic field energy density are expected to produce more robust estimates of the IC emission than previously available. In particular, the implied flat electron spectra $p < 2$, compared to almost all previous models with $p = 2$, has an important impact on the IC emission spectral index and the

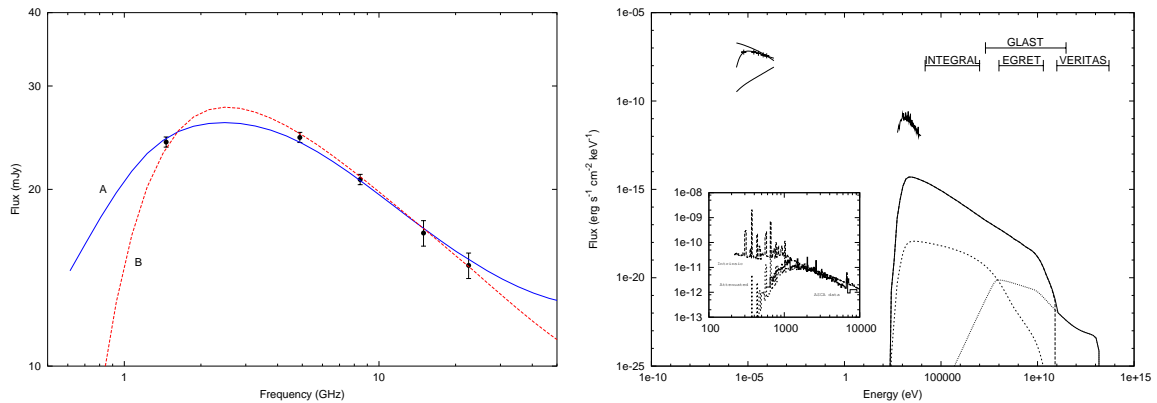


Figure 5: Left: Model fits to radio data of WR 140 at orbital phase 0.837. The observations are the solid circles. The wind-momentum ratio of the two winds is 0.22 (model A) and 0.02 (model B). Equally good fits are possible from both radically different models. Right: The radio, and non-thermal X-ray and γ -ray emission determined from model B, together with the observed radio and X-ray data (from ASCA). The radio model shown indicates the thermal free-free flux (displayed below the data points), the *intrinsic* synchrotron flux before free-free absorption (displayed above the data points), and the observed emission. The model IC (long dash), relativistic bremsstrahlung (short dash), and pion decay (dotted) emission components are shown, along with the total emission (solid). The energy ranges of a number of satellite missions are shown. The insert shows details of model fits to the ASCA thermal X-ray data that is used to constrain the mass-loss rate and momentum ratio of the winds (from [17]).

predicted X-ray and γ -ray flux. In addition to the shock accelerated electrons, it is anticipated that ions will also be accelerated to relativistic energies, giving rise to the possibility of γ -ray emission from pion decay.

Fig. 5 shows a predicted high-energy spectrum for WR140 [17]. IC emission dominates at energies below 50 GeV while pion decay emission is evident above this energy. The nature of the high-energy spectrum is strongly dependent on a number of key properties of the shock acceleration in the WCR. As examples, the cutoff in the IC and pion decay emission is dependent, respectively, on the maximum electron and ion energies that can be attained at the shocks. Also, the luminosity of the IC and pion decay emission are both dependent on the efficiency of electron and ion acceleration at the shocks. Indeed, it has already been possible to rule out several models of the radio data based on the lack of a detection of WR140 by INTEGRAL. It is clear that observations with high-energy emission satellites such as GLAST, AGILE, and Suzuka, and ground-based facilities like VERITAS or MAGIC will provide additional constraints on the shock acceleration process, particularly the acceleration efficiency for ions and electrons, and the spectral index of the non-thermal energy spectrum, p . In turn, these will enable the identification of unique model fits to the radio spectra. This will be especially important for successful modelling of the spectra of WR140 throughout its complete orbit cycle.

4. And what of O-type stars?

Now that the source of synchrotron radio emission, and potentially non-thermal X-ray and γ -ray emission, in WR stars has been established as a WCR, it raises the possibility of also explaining

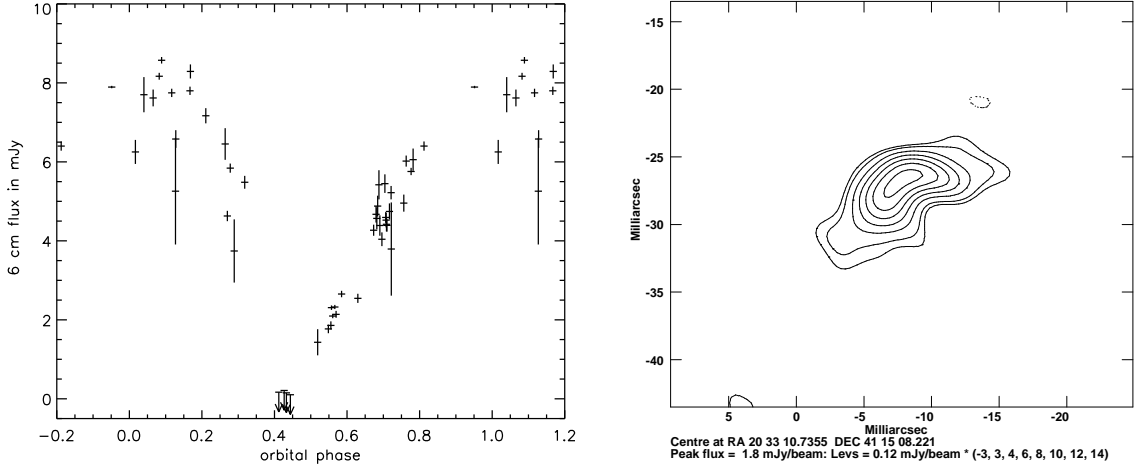


Figure 6: Left: 5-GHz flux of Cyg OB2 #9, modulated by a 2.35-year period, based on a preliminary reduction of archive VLA data. Phase 0.0 was arbitrarily set at radio maximum (S. van Loo, priv. comm.). Right: An 8.4-GHz VLBA observation of Cyg OB2 #9. A bow-shaped WCR is clearly resolved.

synchrotron emission in O-type stars, the progenitors of WR stars. Certainly, of the $\sim 40\%$ of all radio detected O-stars that exhibit non-thermal radio emission, 60% are established binary or multiple systems [24], and a WCR origin for the emission seems certainly plausible.

Alternative mechanisms have been advanced to explain the non-thermal emission in O-type stars. Wind-driven instability shocks e.g. [3], have been demonstrated to be too weak in the outer regions of the wind to produce the necessary relativistic electrons if the electrons are trapped by such shocks and cannot be re-accelerated [25]. Magnetic confinement of the wind plasma has been invoked to explain the hard X-ray properties of the massive stars in the Orion cluster, with the presence of non-thermal radio emission cited as supporting evidence [22]. However, it is certainly clear from high-precision VLBI astrometry that at least in θ^1 Orionis A the non-thermal radio emission is *not* associated with the massive O-type star, but a nearby pre-main sequence star [11]. Clearly, VLBI astrometry is an essential tool in determining the precise location of the non-thermal emission relative to the stars, most especially when many of the associations of stars and non-thermal emission were established initially from relatively low resolution radio imaging carried out with VLA.

The observational support for the CWB model among O-type stars is rising. In the case of Cyg OB2 #5, a 6.6-day binary O6+O6 star system, the synchrotron emission originates from a WCR between the O-star binary and a B-type star ~ 0.9 arcseconds distant [4]. However, there remain several O-type stars that exhibit the characteristics of non-thermal radio emission where a CWB origin for the emission is challenged by the lack of evidence of a companion star. In Cyg OB2 #9, there is no spectroscopic evidence of a binary system, yet analysis of the radio emission from the system shows that the emission is clearly modulated with a 2.35-year period (Fig. 6), similar to the behaviour observed in WR140. If Cyg OB2 #9 is indeed a binary, the secondary must be less luminous than the primary (otherwise it would have been detected in optical spectra) and consequently will have a weaker wind. In that case, a putative WCR should be bow-shaped. VLBA observations of this system reveal that this is indeed the case (Fig. 6), pointing strongly towards a

WCR origin for the emission. The challenge of finding the companion (or companions) that give rise to this WCR remains.

5. Summary

High-resolution radio observations have demonstrated that non-thermal radio emission in WR stars arises where the wind of the WR star collides with that of a massive stellar companion. There is now evidence to suggest that non-thermal emission in O-type stars, the progenitors to WR stars, may also arise from wind collision. In conjunction with hydrodynamic models of the WCR, radiometry and high-resolution VLBI imaging are being used to constrain the particle acceleration process, particularly the electron spectrum and the efficiency of the acceleration process. These models can be used to predict the high-energy emission from the WCR. With the advent of high energy facilities such as GLAST, AGILE, Suzuka, MAGIC, and VERITAS, it will be possible to place further constraints on the acceleration process, which will be important for successful models of the dramatic variations of the emission observed in systems such as WR140.

References

- [1] D. C. Abbott, J. H. Bieging, and E. Churchwell, *The detection of variable, nonthermal radio emission from two O type stars*, ApJ **280**, 671–678 (1984).
- [2] D. C. Abbott, A. V. Torres, J. H. Bieging, and E. Churchwell, *Radio emission from galactic Wolf-Rayet stars and the structure of Wolf-Rayet winds*, ApJ **303**, 239–261 (1986).
- [3] W. Chen and R. L. White, *Nonthermal radio emission from hot star winds: Its origin and physical implications*, Ap&SS **221**, 259–272 (1994).
- [4] M. E. Contreras, L. F. Rodriguez, M. Tapia, D. Cardini, A. Emanuele, M. Badiali, and P. Persi, *Hipparcos, VLA, and CCD Observations of Cygnus OB2 No. 5: Solving the Mystery of the Radio "Companion"*, ApJ **488**, L153–L156 (1997).
- [5] S. M. Dougherty, A. J. Beasley, M. J. Claussen, B. A. Zauderer, and N. J. Bolingbroke, *High-Resolution Radio Observations of the Colliding-Wind Binary WR 140*, ApJ **623**, 447–459 (2005).
- [6] S. M. Dougherty, J. M. Pittard, L. Kasian, R. F. Coker, P. M. Williams, and H. M. Lloyd, *Radio emission models of colliding-wind binary systems*, A&A **409**, 217–233 (2003).
- [7] S. M. Dougherty and P. M. Williams, *Non-thermal emission in Wolf-Rayet stars: are massive companions required?*, MNRAS **319**, 1005–1010 (2000).
- [8] S. M. Dougherty, P. M. Williams, and D. L. Pollacco, *WR 146 - observing the OB-type companion*, MNRAS **316**, 143–151 (2000).
- [9] S. M. Dougherty, P. M. Williams, K. A. van der Hucht, M. F. Bode, and R. J. Davis, *Multifrequency observations of the Wolf-Rayet star WR 146: another colliding-wind binary?*, MNRAS **280**, 963–970 (1996).
- [10] D. Eichler and V. Usov, *Particle acceleration and nonthermal radio emission in binaries of early-type stars*, ApJ **402**, 271–279 (1993).

- [11] S. T. Garrington, H. J. van Langevelde, R. M. Campbell, and A. Gunn, *MERLIN and Global VLBI Observations of θ^1 Orionis A* in proceedings of *Proceedings of the 6th EVN Symposium*, (E. Ros, R. W. Porcas, A. P. Lobanov, and J. A. Zensus, eds.), June 2002, pp. 259–262.
- [12] M. Jardine, H. R. Allen, and A. M. T. Pollock, *Particle acceleration in colliding wind binary systems.*, *A&A* **314**, 594–598 (1996).
- [13] S. V. Marchenko, A. F. J. Moffat, D. Ballereau, J. Chauville, J. Zorec, G. M. Hill, K. Annuk, L. J. Corral, H. Demers, P. R. J. Eenens, K. P. Panov, W. Seggewiss, J. R. Thomson, and A. Villar-Sbaffi, *The Unusual 2001 Periastron Passage in the “Clockwork” Colliding-Wind Binary WR 140*, *ApJ* **596**, 1295–1304 (2003).
- [14] J. D. Monnier, W. A. Traub, F. P. Schloerb, R. Millan-Gabet, J.-P. Berger, E. Pedretti, N. P. Carleton, S. Kraus, M. G. Lacasse, M. Brewer, S. Ragland, A. Ahearn, C. Coldwell, P. Haguenaue, P. Kern, P. Labeye, L. Lagny, F. Malbet, D. Malin, P. Maymounkov, S. Morel, C. Papaliolios, K. Perraut, M. Pearlman, I. L. Porro, I. Schanen, K. Souccar, G. Torres, and G. Wallace, *First Results with the IOTA3 Imaging Interferometer: The Spectroscopic Binaries λ Virginis and WR 140*, *ApJ* **602**, L57–L60 (2004).
- [15] V. S. Niemela, M. M. Shara, D. J. Wallace, D. R. Zurek, and A. F. J. Moffat, *Hubble Space Telescope Detection of Optical Companions of WR 86, WR 146, and WR 147: Wind Collision Model Confirmed*, *AJ* **115**, 2047–2052 (1998).
- [16] E. P. O’Connor, S. M. Dougherty, J. M. Pittard, and P. M. Williams, *The colliding winds of WR 146: seeing the works* in proceedings of *Massive Stars and High-Energy Emission in OB Associations*, (G. Rauw, Y. Nazé, and E.R. Blomme, Gosset, eds.), November 2005, pp. 81–84.
- [17] J. M. Pittard and S. M. Dougherty, *Radio, X-ray, and γ -ray emission models of the colliding-wind binary WR140*, *MNRAS*, 801–826 (2006).
- [18] J. M. Pittard, S. M. Dougherty, R. F. Coker, E. O’Connor, and N. J. Bolingbroke, *Radio emission models of colliding-wind binary systems. Inclusion of IC cooling*, *A&A* **446**, 1001–1019 (2006).
- [19] A. M. T. Pollock, M. F. Corcoran, and I. R. Stevens, *Testing Colliding-Wind X-Ray Theories with WR140* in proceedings of *ASP Conf. Ser. 260: Interacting Winds from Massive Stars*, (A. F. J. Moffat and N. St-Louis, eds.), 2002, pp. 537–545.
- [20] A. M. T. Pollock, M. F. Corcoran, I. R. Stevens, and P. M. Williams, *Bulk Velocities, Chemical Composition, and Ionization Structure of the X-Ray Shocks in WR 140 near Periastron as Revealed by the Chandra Gratings*, *ApJ* **629**, 482–498 (2005).
- [21] G. E. Romero, P. Benaglia, and D. F. Torres, *Unidentified 3EG gamma-ray sources at low galactic latitudes*, *A&A* **348**, 868–876 (1999).
- [22] B. Stelzer, E. Flaccomio, T. Montmerle, G. Micela, S. Sciortino, F. Favata, T. Preibisch, and E. D. Feigelson, *X-Ray Emission from Early-Type Stars in the Orion Nebula Cluster*, *ApJS* **160**, 557–581 (2005).
- [23] K. A. van der Hucht, P. M. Williams, T. A. T. Spocłstra, and A. C. de Bruyn, *Non-Thermal Radio Observations of Wolf-Rayet Stars: A Case for Long-Period Binaries (Invited Paper)* in proceedings of *ASP Conf. Ser. 22: Nonisotropic and Variable Outflows from Stars*, (L. Drissen, C. Leitherer, and A. Nota, eds.), 1992, pp. 249–268.
- [24] S. van Loo, *Non-thermal radio emission from single*, Ph.D. Thesis (2005).
- [25] S. van Loo, M. C. Runacres, and R. Blomme, *Can single O stars produce non-thermal radio emission?*, *A&A* **452**, 1011–1019 (2006).

- [26] R. L. White and R. H. Becker, *An Eight-Year Study of the Radio Emission from the Wolf-Rayet Binary HD 193793 = WR 140*, ApJ **451**, 352–358 (1995).
- [27] P. M. Williams, S. M. Dougherty, R. J. Davis, K. A. van der Hucht, M. F. Bode, and D. Y. A. Setia Gunawan, *Radio and infrared structure of the colliding-wind Wolf-Rayet system WR147*, MNRAS **289**, 10–20 (1997).
- [28] P. M. Williams, K. A. van der Hucht, A. M. T. Pollock, D. R. Florkowski, H. van der Woerd, and W. M. Wamsteker, *Multi-frequency variations of the Wolf-Rayet system HD 193793. 1 - Infrared, X-ray and radio observations*, MNRAS **243**, 662–684 (1990).
- [29] P. M. Williams, K. A. van der Hucht, and T. A. T. Spoelstra, *Multi-frequency variations of the Wolf-Rayet system HD 193793. 2: Observations of the 1991-92 radio maximum*, A&A **291**, 805–810 (1994).
- [30] S. A. Zhekov and S. L. Skinner, *X-Ray Emission from Colliding Wind Shocks in the Wolf-Rayet Binary WR 140*, ApJ **538**, 808–817 (2000).